Initial studies on mechanism of action and cell death of active *N*-oxide-containing heterocycles in *Trypanosoma cruzi* epimastigotes *in vitro*

DIEGO BENÍTEZ[1], GABRIELA CASANOVA[2], GONZALO CABRERA[3], NORBEL GALANTI[3], HUGO CERECETTO[1]* *and* MERCEDES GONZÁLEZ[1]*

[1] *Grupo de Química Medicinal, Laboratorio de Química Orgánica, Facultad de Ciencias-Facultad de Química, Universidad de la República, Montevideo, Uruguay*
[2] *Unidad de Microscopía Electrónica de Transmisión, Facultad de Ciencias, Universidad de la República, Montevideo, Uruguay*
[3] *Facultad de Medicina, Programa de Biología Celular y Molecular, Instituto de Ciencias Biomédicas, Universidad de Chile, Santiago, Chile*

(*Received 8 August 2013; revised 11 October and 19 October 2013; accepted 21 October 2013; first published online 27 January 2014*)

SUMMARY

Chagas disease, endemic in 21 countries across Latin America, kills more people in the region each year than any other parasite-borne disease. Therapeutic options have problems ranging from toxicity, poor efficacy, drug resistance and high cost. Thus, cheaper and less toxic treatments are necessary. From our in-house chemical library of agents against *Trypanosoma cruzi* the most relevant *N*-oxide-containing heterocycles were selected for mode of action and type of death studies. Also included in these studies were two active nitrofuranes. Epimastigotes of *T. cruzi* were used as the biological model in this study. The metabolic profile was studied by ^{1}H NMR in association with the MTT assay. Excreted catabolites data, using ^{1}H NMR spectroscopy, showed that most of the studied *N*-oxides were capable of decreasing both the release of succinate and acetate shedding, the compounds therefore possibly acting on mitochondria. Only quinoxalines and the nitrofurane **Nf1** showed significant mitochondrial dehydrogenase inhibitions, but with different dose–time profiles. In the particular case of quinoxaline **Qx2** the glucose uptake study revealed that the integrity of some pathways into the glycosome could be affected. Optic, fluorescence (TUNEL and propidium iodide) and transmission electron microscopy (TEM) were employed for type of death studies. These studies were complemented with ^{1}H NMR to visualize mobile lipids. At low concentrations none of the selected compounds showed a positive TUNEL assay. However, both quinoxalines, one furoxan and one benzofuroxan showed a necrotic effect at high concentrations. Curiously, one furoxan, **Fx1**, one benzofuroxan, **Bfx1**, and one nitrofurane, **Nf1**, caused a particular phenotype, with a big cytoplasmatic vacuole being observed while the parasite was still alive. Studies of TEM and employing a protease inhibitor (3-methyladenine) suggested an autophagic phenotype for **Bfx1** and **Nf1** and a 'BigEye' phenotype for **Fx1**.

Key words: *Trypanosoma cruzi*, Chagas disease, *N*-oxides, necrosis, autophagy, NMR.

INTRODUCTION

Chagas disease, or American trypanosomiasis, caused by the protozoan *Trypanosoma cruzi* is the largest parasitic disease burden in the American continent affecting approximately 8 million people from the southern USA to northern Chile. Even though the enforcement of public health programmes towards vector elimination in some Latin American countries has decreased the incidence of new infections, the disease is still endemic in large areas (WHO, 2013).

The current treatment of Chagas disease depends on two nitroheterocycles, nifurtimox (Nfx, Fig. 1) and benznidazole. Although effective for acute infections both drugs are not efficient in chronic infections and cause undesirable side effects; therefore, there is an urgent need for the development of safe and effective drugs (Cerecetto and González, 2010). Extensive efforts have been directed to the development of new chemotherapeutic agents but they have been deficient in the final stages of drug development studies, i.e. tolerance/safety, selectivity, drug-resistance, scaling-up, pharmacokinetic and pharmacodynamic properties (González and Cerecetto, 2011).

In an ongoing effort to discover new anti-*T. cruzi* agents, our group has been exploring the moiety *N*-oxide as a pharmacophore for this kind of drug (Cerecetto and González, 2008; Boiani *et al*. 2010). Within this framework, we have investigated the trypanosomicidal activity of different *N*-oxide-containing heterocycles, and from 200 synthesized compounds, two furoxans, i.e. **Fx1**, and **Fx2**, two

* Corresponding authors: Grupo de Química Medicinal, Laboratorio de Química Orgánica, Facultad de Ciencias-Facultad de Química, Universidad de la República, Iguá 4225, 11400 Montevideo, Uruguay. E-mail: megonzal@fq.edu.uy and hcerecetto@cin.edu.uy

doi:10.1017/S003118201300200X

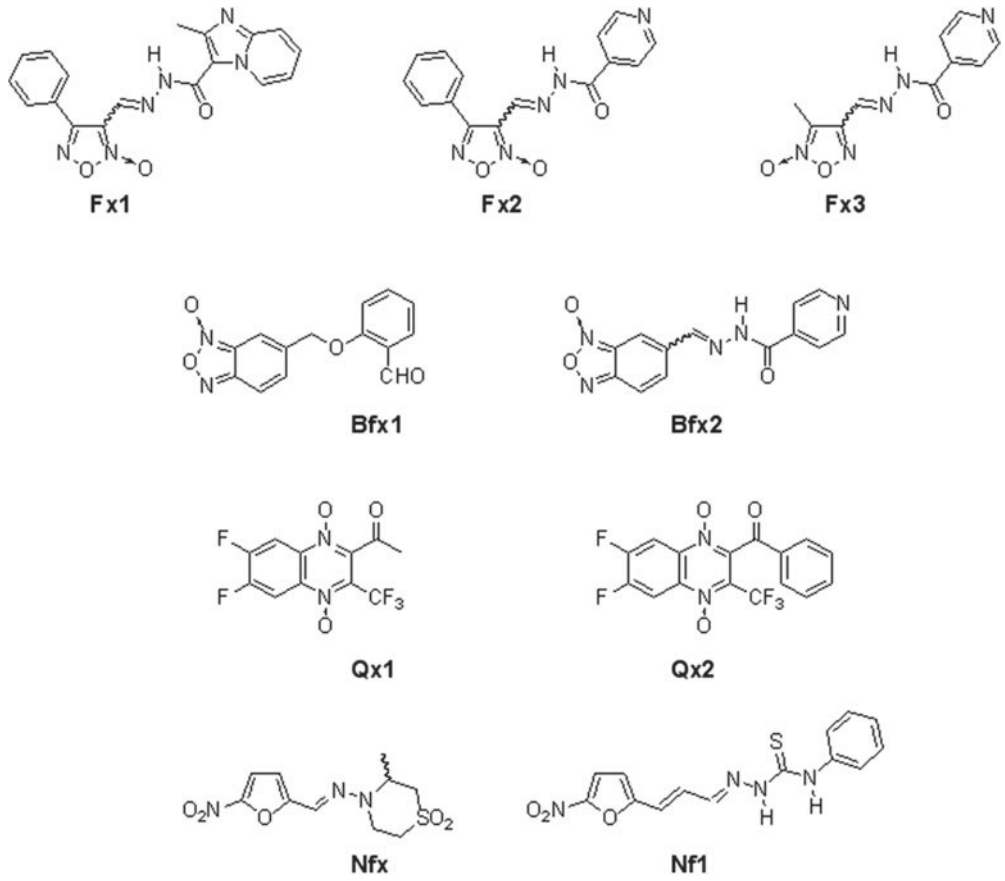

Fig. 1. Chemical structures of the compounds herein studied: *N*-oxide-containing heterocycles (**Fx1**, **Fx2**, **Fx3**, **Bfx1**, **Bfx2**, **Qx1**, **Qx2**), Nifurtimox (**Nfx**) and nitrofurane (**Nf1**).

benzofuroxans, i.e. **Bfx1**, and **Bfx2**, and two quinoxaline 1,4-dioxides, i.e. **Qx1**, and **Qx2** (Fig. 1), were selected based on their excellent *in vitro* activities (Merlino *et al*. 2010; Benítez *et al*. 2011; Hernández *et al*. 2013). Those agents were active on *T. cruzi* epimastigotes, trypomastigotes and intracellular amastigotes from different parasite strains, i.e. Tulahuen 2, Y, Colombiana and the CL Brener clone. Additionally, **Fx1**, **Fx2**, **Qx1** and **Qx2** did not exhibit mutagenicity in the Ames test and displayed adequate *in vivo* behaviour in an acute model of Chagas disease (Benítez *et al*. 2011; Hernández *et al*. 2013).

Whereas some efforts have been made to elucidate the mode of action of this kind of compounds, knowledge on this subject is still incomplete. Thus, it has been demonstrated that some benzofuroxans, analogues of **Bfx1** and **Bfx2**, are strong inhibitors of parasite dehydrogenase activity affecting mitochondrial membrane potential (Boiani *et al*. 2010). Accordingly we have proved that **Qx1** and **Qx2**, in contrary to **Nfx**, decrease mitochondrial dehydrogenase activity thus diminishing the excreted catabolites acetate and succinate in the parasite (Benítez *et al*. 2011). New knowledge about the mode of action of these kinds of compounds (Fig. 1) may lead to the discovery of new drug targets that help overcome problems related to drug toxicity and drug resistance.

Among the different strategies that have been used to elucidate the mechanism of action of anti-*T. cruzi* drugs (De Castro and Meirelles, 1990; Menna-Barreto *et al*. 2010) we have successfully applied ^{1}H NMR for the evaluation of *T. cruzi*-excreted catabolites (Boiani *et al*. 2008; Caterina *et al*. 2008; Benítez *et al*. 2011).

Studies on the parasite death phenotype when treated with these compounds are have not been done. This aspect is relevant considering that, for other pathologies and drugs, such knowledge is leading to the design of novel drugs targeting critical points in the death process (Ricci and Zong, 2006; MacKenzie and Clark, 2008; Tan and White, 2008). Different cell death phenotypes caused by chemotherapeutic agents have been described in *T. cruzi* (Menna-Barreta *et al*. 2009*a*). Interestingly, in protozoa a variety of drug stimuli converge to the same pathway of death, suggesting an intense crossover between the three types of programmed cell death (PCD), i.e. apoptosis (type I PCD), autophagy (type II PCD) and programmed necrosis (type III PCD). Different techniques have been employed in the study of *T. cruzi* cell death, i.e. destructive techniques such as flow cytometry, fluorescence microscopy, Western blot, agarose-gel electrophoresis and ultrastructural analysis, or less destructive ones such as protease inhibition analysis (Alvarez *et al*.

2008*a*, *b*; Jiménez *et al*. 2008; Irigoín *et al*. 2009; Menna-Barreto *et al*. 2009*a*). Recently, we have described the use of ^{1}H NMR spectroscopy (Benítez *et al*. 2012) as a non-invasive method that allows the visualization of the phenomenon of mobile lipid accumulation following the induction of either apoptosis or cytostasis.

The aim of the present study was to analyse some aspects of the mode of action and cell death phenotype induced by the *N*-oxides shown in Fig. 1. The results indicated a clear difference in the mechanism of action of the newly studied *N*-oxides compared with the previous ones (Boiani *et al*. 2010) and particular cell death pathways, for some of them, unrelated to the kind of *N*-oxide.

MATERIALS AND METHODS

Chemicals

N-oxides **Fx1**, **Fx2**, **Fx3**, **Bfx1**, **Bfx2**, **Qx1** and **Qx2** as well as the nitrofurane, **Nf1** (Fig. 1), were obtained as previously described (Merlino *et al*. 2010; Aravena *et al*. 2011; Benítez *et al*. 2011; Hernández *et al*. 2013). **Nfx** was purchased from Bayer. Other chemicals were purchased from Sigma-Aldrich unless otherwise indicated.

Cell cultures

Trypanosoma cruzi epimastigote forms (Y strain) were cultured at 28 °C for 5–7 days (exponential phase of growth) under aerobiosis in axenic BHI-tryptose milieu (33 g L^{-1} brain-heart infusion, 3 g L^{-1} tryptose, 0·02 g L^{-1} hemin, 0·3 g L^{-1} D-(+)-glucose, supplemented with 10% (v/v) calf serum, 200 000 units L^{-1} penicillin and 0·2 g L^{-1} streptomycin). For TUNEL and PI-staining studies, *T. cruzi* epimastigote forms (Y strain and CL Brener clone) were cultured at 28 °C for 5–7 days (exponential phase of growth) under aerobiosis in axenic Diamond milieu (12·5 g L^{-1} yeast extract, 12·5 g L^{-1} tryptose, 12·5 g L^{-1} tryptone, 106 mM NaCl, 29 mM H_2KPO_4, 23 mM HK_2PO_4, 7·2 pH, 7·5 mM hemin supplemented with 10% (v/v) calf serum, 75 units mL^{-1} penicillin and 75 mg L^{-1} streptomycin).

^{1}H NMR study of the excreted catabolites

For ^{1}H NMR spectroscopic studies, parasites in exponential phase of growth are resuspended in fresh milieu. One mL containing 10 million *T. cruzi* (Y strain) treated for 2 days with each studied compound at the IC_{50} doses (**Fx1** 14·8 ± 2·2 μM, **Fx2** 7·95 ± 0·06 mM, **Bfx1** 4·8 ± 0·6 mM, **Bfx2** 13·3 ± 0·1 mM, **Qx1** 1·6 ± 0·4 mM, **Qx2** 1·8 ± 0·1 mM, **Nfx** 6·5 ± 0·2 mM, **Nf1** 1·3 ± 0·5 mM and **Fx3** >300·0 mM,), were centrifuged at 3000 ***g*** for 10 min. Before measuring, 0·01 mL of DMF, as internal standard, and 0·09 mL of D_2O were added to 0·5 mL of the supernatant. Spectra were registered with water suppression in 5 mm NMR (Aldrich, USA) sample tubes. The chemical displacements used to identify the respective metabolites were previously confirmed by adding each analysed metabolite to the studied supernatant as well as by a control solution with 4 mg mL^{-1} of each metabolite in buffer phosphate, pH = 7·4. Each run was done, at least, in triplicate and Student's *t*-test was used to analyse the significance of the changes. The chemical shifts (δ, ppm) and multiplicity of the analysed catabolites are: Lac, 1.316, d; Ala, 1.466, d; Ace, 1.904, s; Pyr, 2.357, s; Suc, 2.392, s; Gly, 3.547, s. For quinoxaline di-*N*-oxides, **Qx1** and **Qx2**, a dose–response study was performed using IC_{50}, $3 \times IC_{50}$ and $5 \times IC_{50}$. Two controls were used, a control with fresh milieu and a control with parasites, with the corresponding concentration of parasites and DMSO used in the samples.

Mitochondrial dehydrogenase activities

Mitochondrial dehydrogenase activities were measured in 24-well plates. Twenty million per mL *T. cruzi* epimastigotes (Y strain) were washed twice at 3000 ***g*** for 10 min and resuspended in PBS-glucose (5·5 μM). Then 600 μL were loaded in each well and 20 mM of each of the studied compounds were added. The assay was performed in quadriplicate and untreated parasites were maintained as controls corresponding to the given time of treatment. The cultures were incubated at 28 °C. At different incubation times the epimastigotes were counted and the colorimetric MTT dye-reduction assay was performed. For this purpose, 25 μL of a solution containing 4 mg mL^{-1} of MTT in PBS-glucose (5·5 mM) were added to each well and plates were incubated for an additional 2 h at 28 °C. The reaction was stopped by the addition of 100 μL SDS-isopropanol (10% SDS, 50% isopropanol, H_2O) and incubated for an additional 2 h at 28 °C. The absorbance was measured at 570 nm. Under these conditions, compounds did not interfere with the reaction mixture. Percentage of mitochondrial dehydrogenase activities (Pmdh) were determined using untreated parasites' activities as 100%.

Glucose uptake studies (*Boiani* et al. 2009)

Trypanosoma cruzi epimastigotes (Y strain, 100×10^6 parasites mL^{-1}) were washed twice with PBS-glucose and resuspended in PBS-glucose (5·5 mM). 800 μL of this suspension were transferred to a 24-well cell-culture plate. Then, **Qx2** was added dissolved in DMSO (8 μL), at IC_{50} and $3 \times IC_{50}$ concentrations and incubated for 4 h. After centrifugation at 3000 ***g*** for 10 min the parasite-free supernatant was treated with 500 μL Benedict's reagents at

reflux during 5 min. Glucose concentration was determined, measuring at 744 nm using a calibration curve. Negative controls were made with DMSO or **Qx2** at IC_{50} and $3 \times IC_{50}$.

Cell death phenotype studies

^1H NMR-VML spectroscopy analysis

Cell sample preparation. Treated or un-treated (control) cells (150×10^6) were harvested and centrifuged for 10 min at 3000 ***g***. The pellet was washed three times in PBS, re-suspended in PBS (500 μL), transferred to a 5 mm NMR tube (ALDRICH, USA) and D_2O (90 μL) was added. The mixture was homogenized prior to acquire the spectrum.

NMR spectra acquisition. ^1H NMR experiments were recorded at 20 °C in a Bruker Avance DPX-400 spectrometer, operating at 400·132 mHz, with a 5 mm broadband inverse geometry probe. The acquisition parameters were 90° pulse (zgpr, avance-version v 1.7.10.2, 1D sequence with f1 presaturation), 128 scans, and spectral width of 14·983 ppm. The acquisition time was 1·3664 s. Signal intensities were calculated by performing appropriate baseline corrections and then integrating the area under each of the resonances using MestRe-C NMR software (http://mestrelab.com/). Spectra were analysed using the Topspin 1.3 software package. The integrated regions were 1·20–1·35 ppm for CH_2 and 0·80–0·90 ppm for CH_3. The visualized regions were 3·10–3·30 ppm for Cho and 2·80 and 5·40 ppm for polyunsaturated fatty acids (PUFA).

Statistical analysis. Values are expressed as means ± S.E.M. of at least three independent experiments. Statistical comparisons were performed with unpaired Student's *t*-tests by using OriginPro 8 software. $P < 0{\cdot}05$ was considered statistically significant.

TUNEL assay and staining with PI. After each treatment parasites (600 μL, 10×10^6 mL^{-1}) were collected by centrifugation at 3000 ***g***, washed twice in PBS, resuspended in the same buffer and placed on a slide. After drying at room temperature the cells were fixed with methanol (70%) and washed in PBS. For TUNEL assays cells were made permeable with 0·2% Triton X-100. Afterwards, cells were incubated with a reaction mix containing dUTP-FITC (Fluorescein isothiocyanate). Nuclei were counterstained with DAPI (4′,6-diamidin-2-phenylindol) (1 mg mL^{-1}). Treatment of parasites with H_2O_2 (500 μM, 30 min of incubation at 28 °C) was included as a positive control (Benítez *et al*. 2012) and parasites without treatment were included as a negative one.

For PI-staining, after the permeabilization step 30 μL of PI solution (1 μg mL^{-1}) was added, mixed and immediately observed at 400× using Nikon Eclipse E400 microscopy fluorescence-microscopy. Pictures were captured with a Nikon Coolpix 4500 digital camera. Results were quantified counting 200 cells in duplicate from three independent experiments.

Ultrastructural analysis. Parasites treated with **Fx1**, **Bfx1** or **Nf1** were processed for TEM analysis. After washing three times in PBS, the parasites (an optimum amount of 400×10^6) were fixed in 2·5% glutaraldehyde (40 min/room temperature) and post-fixed in a solution containing 1% OsO_4, 0·8% potassium ferricyanide and 2·5 mM $CaCl_2$ (30 min/room temperature). Afterwards the cells were dehydrated in an ascending alcohol series following by acetone and embedded in epoxy-resin (Araldita Durcupan, FLUKA). Thin sections, 0·5 μM, were stained with methyleneboraxic blue (1%) and examined in a Nikon Eclipse E200 microscope. Ultrathin sections were stained with uranyl acetate and lead citrate during 10 min and examined in a Jeol JEM 1010 transmission microscope operated at 80 kV. Controls for autophagy (starved parasites in PBS for 24 h) (Benítez *et al*. 2012) and normal parasites (parasites incubated with the compounds dissolvent, DMSO) were included.

Protease inhibition analysis. Epimastigotes (10 million mL^{-1}, strains Y or Tulahuen 2) were incubated for 2 h with the protease inhibitor 3-methyladenine (3-MA, 20 mM, Sigma-Aldrich) at 28 °C. Afterwards, the parasites were washed with PBS (3× at 3000 ***g*** for 10 min), resuspended in culture milieu, and incubated with **Fx1**, **Bfx1** or **Nf1** at 28 °C. Cell quantification was performed using a Neubauer chamber during 5 days. Three independent experiments were performed. Untreated parasites were used as control.

RESULTS

Effect of N*-oxides on* T. cruzi *epimastigotes-excreted catabolites by ^1H NMR*

Parasite-excreted catabolites in presence of *N*-oxides could give information on the biological pathways affected by these compounds. Consequently, we assayed this parameter by ^1H NMR spectroscopy. This technique has proved to be a useful tool in the elucidation of the mechanism of drug action (Sánchez-Moreno *et al*. 1995; Mesa-Valle *et al*. 1996; Fernandez-Ramos *et al*. 1999; Boiani *et al*. 2008; Caterina *et al*. 2008; Benítez *et al*. 2011; Sánchez-Moreno *et al*. 2012).

For that purpose we compared the ^1H NMR spectra of supernatants from the parasites treated with *N*-oxides **Fx1**, **Fx2**, **Bfx1**, **Bfx2**, **Qx1** and **Qx2** with those from untreated *T. cruzi* epimastigotes (Y strain) and from Nfx, the inactive *N*-oxide **Fx3**

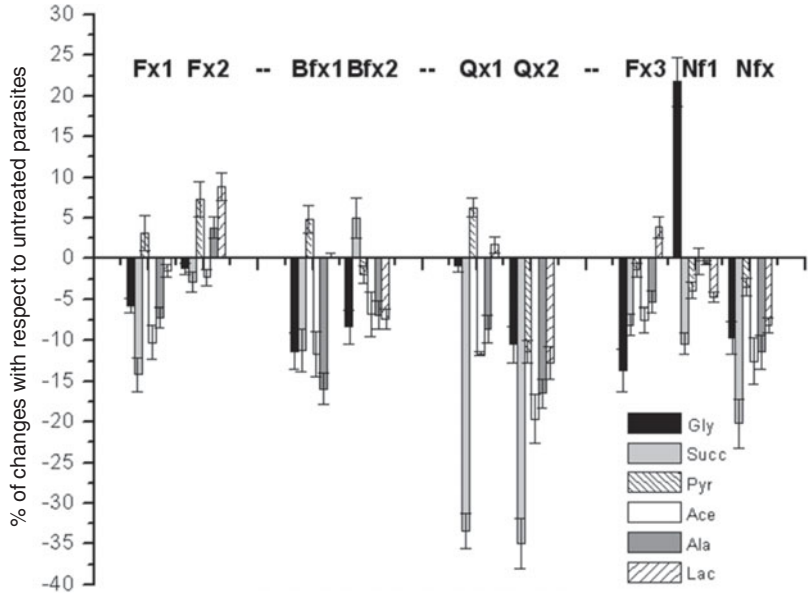

Fig. 2. Percentage of the end products excreted by *T. cruzi* epimastigote Y strain to the milieu expressed with respect to untreated parasites.

and the active nitrofurane Nf1 (Fig. 1). All compounds were tested at their IC_{50}, except for compound **Fx3** that was assayed at 300 μM because its IC_{50} was not determined due to solubility problems. We have mainly focused on the carboxylic acid salts lactate (Lac), acetate (Ace), pyruvate (Pyr) and succinate (Succ) and on alanine (Ala) and glycine (Gly), which are the most relevant modified catabolites (Fig. 2).

With the exception of nitrofurane **Nf1** all the *N*-oxides decreased the excreted Gly and Ace. The most effective compound in reducing the amount of released Gly was the furoxan **Fx3** while the quinoxaline di-*N*-oxide **Qx2** induced a marked decrease of Ace. All compounds, except **Bfx2**, decreased the release of Succ, the best inhibitors being the quinoxalines **Qx1** and **Qx2** (Benítez *et al*. 2011). Regarding the release of Pyr no pattern was observed; this catabolite increased after incubation of parasites with **Fx1**, **Fx2**, **Bfx1** and **Qx1** while it diminished when treated with **Fx3**, **Bfx2** and **Qx2**. Benzofuroxans and quinoxaline di-*N*-oxides decreased the amount of excreted Ala, with **Bfx1** and **Qx2** being the most active. Two furoxans, **Fx2** and **Fx3**, increased the amount of released Lac while no significantly increase in the concentration of release Lac was observed after incubation of parasites with the rest of the heterocycles containing *N*-oxides. When dose–response studies were performed with quinoxaline di-*N*-oxides a decrease of Lac was observed for both derivatives, **Qx1** and **Qx2**, at a dose five-fold the corresponding IC_{50} (Fig. 3), with **Qx2** being the best inhibitor of Lac-release. A clear dose–response was observed for the inhibition of Gly, Succ and Ace excretion. Figure 4 shows representative examples of the spectra generated for selected compounds.

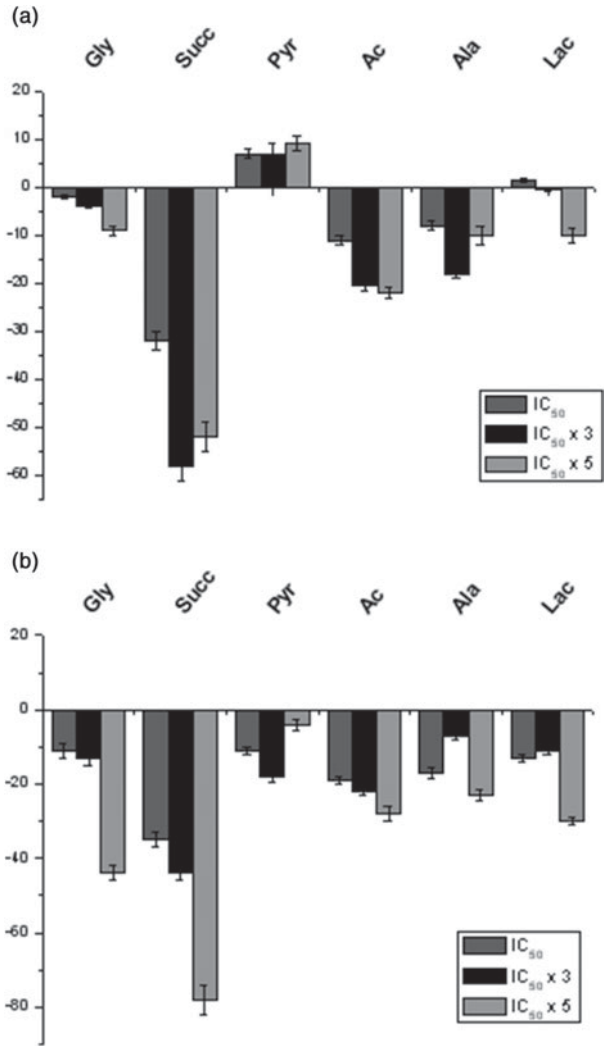

Fig. 3. Catabolites excreted by parasites treated with compounds **Qx1** (a) and **Qx2** (b). Dose–response studies.

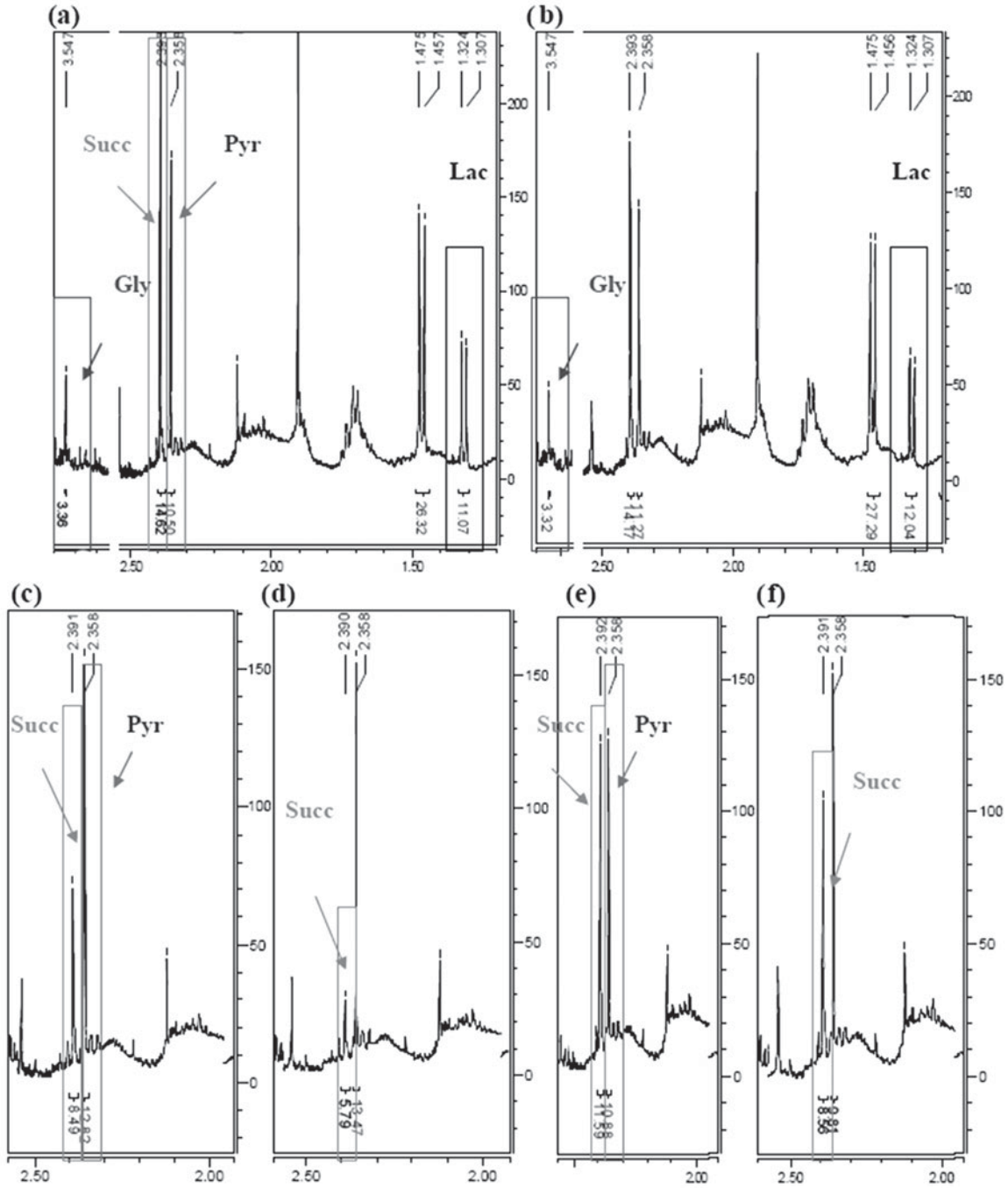

Fig. 4. Relevant regions of the ^{1}H NMR spectra for the assayed excreted-catabolites. (a), (c) and (e) Untreated-parasites; (b), (d) and (f) Parasites treated with **Fx2**, **Qx1** and **Qx2** at its IC_{50}, respectively. For experimental details see Materials and methods section. All the spectra were recorded in D_2O at 295·16 K. Relevant changes in catabolite concentrations are highlighted.

Effect of N*-oxides on mitochondrial dehydrogenases*

Since most of the studied *N*-oxides were capable of decreasing both the release of Succ and the release of Ace, we studied the effect of *N*-oxides on mitochondrial dehydrogenases. Succ biochemical pathway in the mitochondrion involves a succinate dehydrogenase (complex II-respiratory chain) while Ace requires Succ and the action of an acetate-succinate CoA transferase (Bringaud *et al*. 2006; Opperdoes and Coombs, 2007).

Mitochondrial dehydrogenase activities (Pmdh) for live parasites treated with 20 μM of different *N*-oxides with respect to untreated control was assessed using the MTT assay performed at a short incubation period, no more than 120 min; this procedure was previously described for *Leishmania* (Maarouf *et al*. 1997). The following compounds were tested: active *N*-oxides **Fx1**, **Fx2**, **Bfx1**, **Bfx2**; quinoxalines **Qx1**, **Qx2**; **Nfx** (Benítez *et al*. 2011) as the reference drug; and inactive furoxan **Fx3** and nitrofurane **Nf1** (Table 1). Only the nitrofurane **Nf1**, and unlike the

Table 1. Mitochondrial dehydrogenase activities, as a percentage of untreated parasites, in live parasites treated with the studied *N*-oxides and reference compounds

	Pmdh (%)			
Compound/time (min)	30	60	90	120
Fx1	84·0 ± 1·7	88·5 ± 2·0	92·7 ± 1·0	94·6 ± 1·4
Fx2	87·4 ± 0·6	69·6 ± 1·6	100 ± 1	99·1 ± 1·1
Bfx1	77·5 ± 1·2	90·0 ± 0·7	87·9 ± 2·5	77·9 ± 3·0
Bfx2	86·8 ± 0·3	89·9 ± 0·7	100·0 ± 1·6	100·0 ± 0·6
Qx1[a]	91·1 ± 2·3	62·9 ± 4·5	39·5 ± 4·1	40·3 ± 7·4
Qx2[a]	69·7 ± 2·6	69·6 ± 2·4	70·3 ± 1·8	46·1 ± 8·4
Nfx[a]	91·2 ± 1·2	100·0 ± 0·7	98·5 ± 2·1	100·0 ± 0·9
Nf1	100·0 ± 2·8	82·2 ± 2·5	55·4 ± 7·2	50·0 ± 2·5
Fx3	90·3 ± 0·7	89·1 ± 0·4	100 ± 1	100 ± 0·9

[a] Previously studied (Benítez *et al*. 2011).

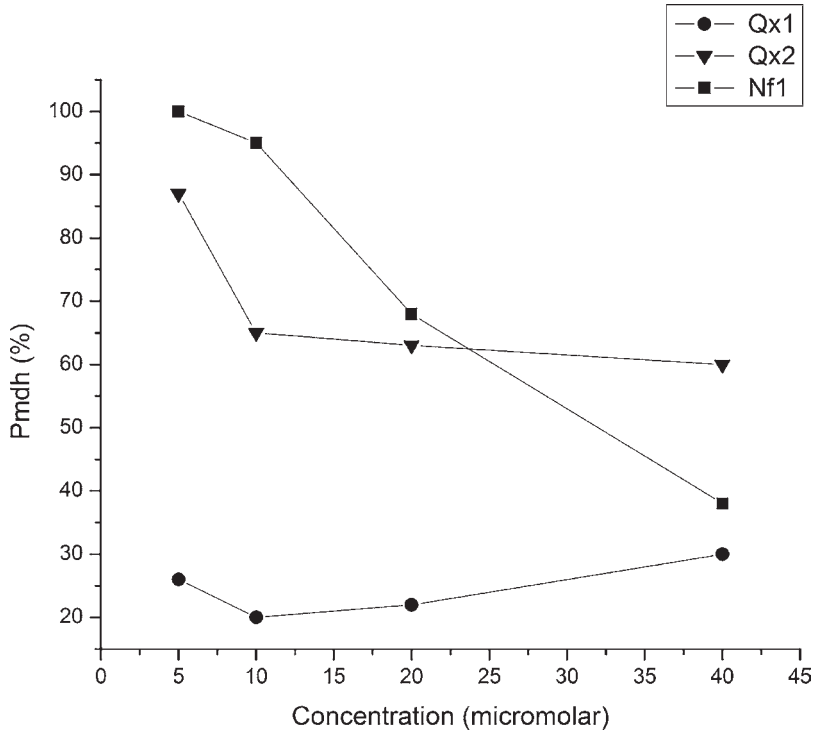

Fig. 5. Mitochondrial dehydrogenases inhibition by **Qx1** (●), **Qx2** (▲) and **Nf1** (■). The enzymatic activities were determined at 90 min of incubation. For experimental details see Materials and methods.

nitrofurane **Nfx**, significantly decreased the mitochondrial dehydrogenase activity in a time-dependent manner while the benzofuroxan Bfx1 showed a moderate effect. A dose–response study was performed with **Qx1**, **Qx2** and **Nf1** using a 90 min incubation time because it was the time at which a more significant change in Pmdh was observed (Fig. 5). Curiously, compounds showing similar IC_{50} against *T. cruzi* (**Qx1** 1·6 ± 0·4 mM, **Qx2** 1·8 ± 0·1 mM and **Nf1** 1·3 ± 0·5 mM) showed different behaviours regarding mitochondrial dehydrogenases, with **Qx1** being an absolute inhibitor at all the assayed doses.

Effect of Qx2 on glucose uptake

Since quinoxaline **Qx2** was able to decrease the release of Succ, Ace, Ala and Lac we studied the ability of this compound to modify glucose uptake by *T. cruzi* epimastigotes. The consumption of glucose by epimastigotes of *T. cruzi* is characterized by the excretion, under aerobic conditions, of reduced products such as Succ, Ace and Ala (Cazzulo, 1992). On the other hand, most trypanosomatids produce Lac from glucose although often as a minor end product, i.e. bloodstream trypomastigotes, and additionally Lac excretion is considerably reduced in mutants showing a reduced glucose consumption rate (Coustou *et al*. 2005).

The glucose uptake (glu-upt) for live parasites treated with the quinoxaline **Qx2**, at the corresponding IC_{50} and at $3 \times IC_{50}$ doses, was assessed using the colorimetric Benedict assay performed at 4 h of incubation (Boiani *et al*. 2009). Clearly, **Qx2** diminished the glucose uptake to 33% at the IC_{50} dose

Table 2. Changes in the visible mobile lipids of *T. cruzi* treated with the different studied compounds analysed by ^{1}H NMR

Compound	Dose (μM)[b]	Time of exposition (h)[b]	Changes in the ^{1}H NMR signals[a]		
			CH_2/CH_3 ratio[c]	'Choline region'	'PUFAs regions'
Fx1	45	24	0·89 ± 0·15	n.m.[d]	n.m.
Fx2	200	24	0·65 ± 0·09	Appearance of PTC, PC, and Cho	n.m.
Bfx1[e]	65	24	1·00 ± 0·16	Increase of Cho	l.m.[f]
Bfx2	200	48	0·87 ± 0·09	Increase of Cho	n.m.
Qx2	200	2	0·70 ± 0·02	d.s.[g]	n.m.
Nfx	300	48	0·98 ± 0·05	d.s.	n.m.
Nf1	13·0	24	0·96 ± 0·19	n.m.	n.m.
Fx3	300·0	24	0·77 ± 0·17	n.m.	n.m.

[a] Respect to untreated parasites.
[b] The doses and time of exposition was determined for each compound using light microscopy.
[c] Expressed respect to untreated parasites.
[d] 'n.m.': not detected modifications.
[e] Using Tulahuen 2 strain.
[f] 'l.m.': little modifications.
[g] 'd.s.': disappearance or decrease of signals.

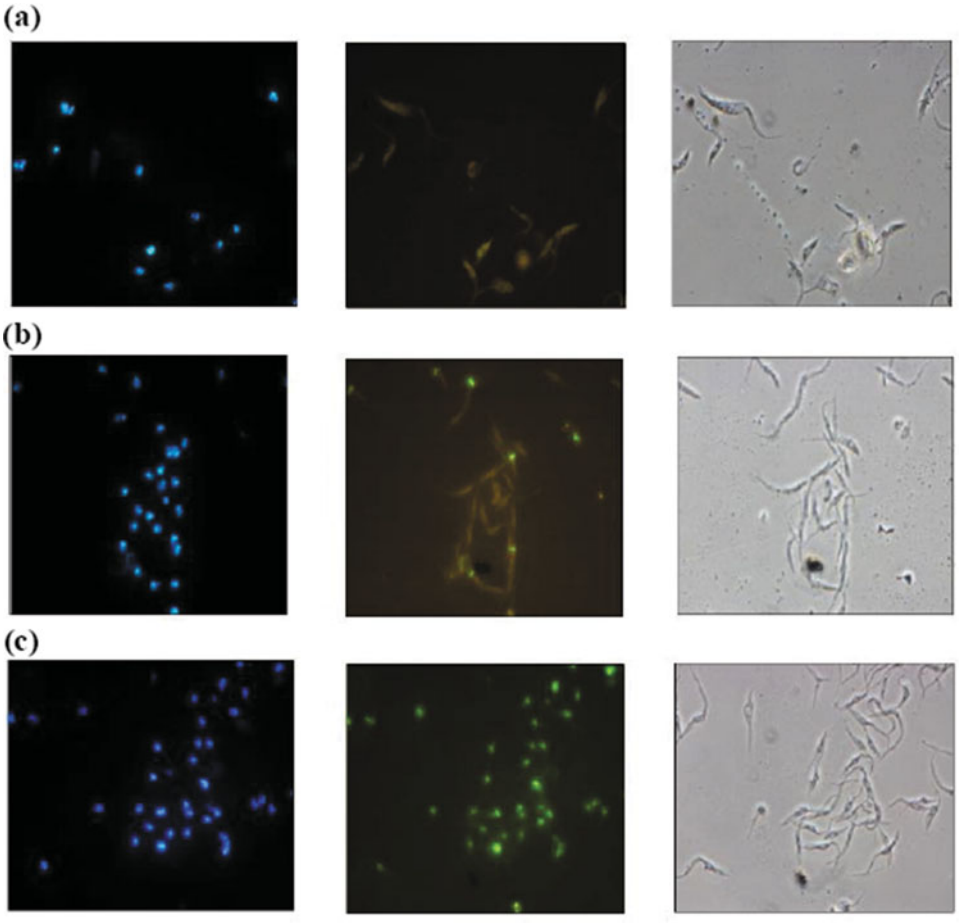

Fig. 6. TUNEL assays (left, DAPI-staining; centre, FITC-staining; right, phase contrast; 1000×). (a) Treatment with **Bfx1** (72 μM, 24 h); (b) Treatment with **Nf1** (19·5 μM, 48 h); (c) Positive control (H_2O_2: 500 μM, 30 min of incubation at 28 °C).

(1·9 mM glu-upt compared with 3·0 mM glu-upt when DMSO was used). Contrarily, at a dose three times the IC_{50} an increase in glucose was observed, probably as a result of the loss of cellular integrity promoted by this high *N*-oxide concentration (− 1·3 mM glu-upt compared with 3 mM glu-upt when DMSO was used). These results are in agreement with the ^{1}H NMR study of excreted catabolites.

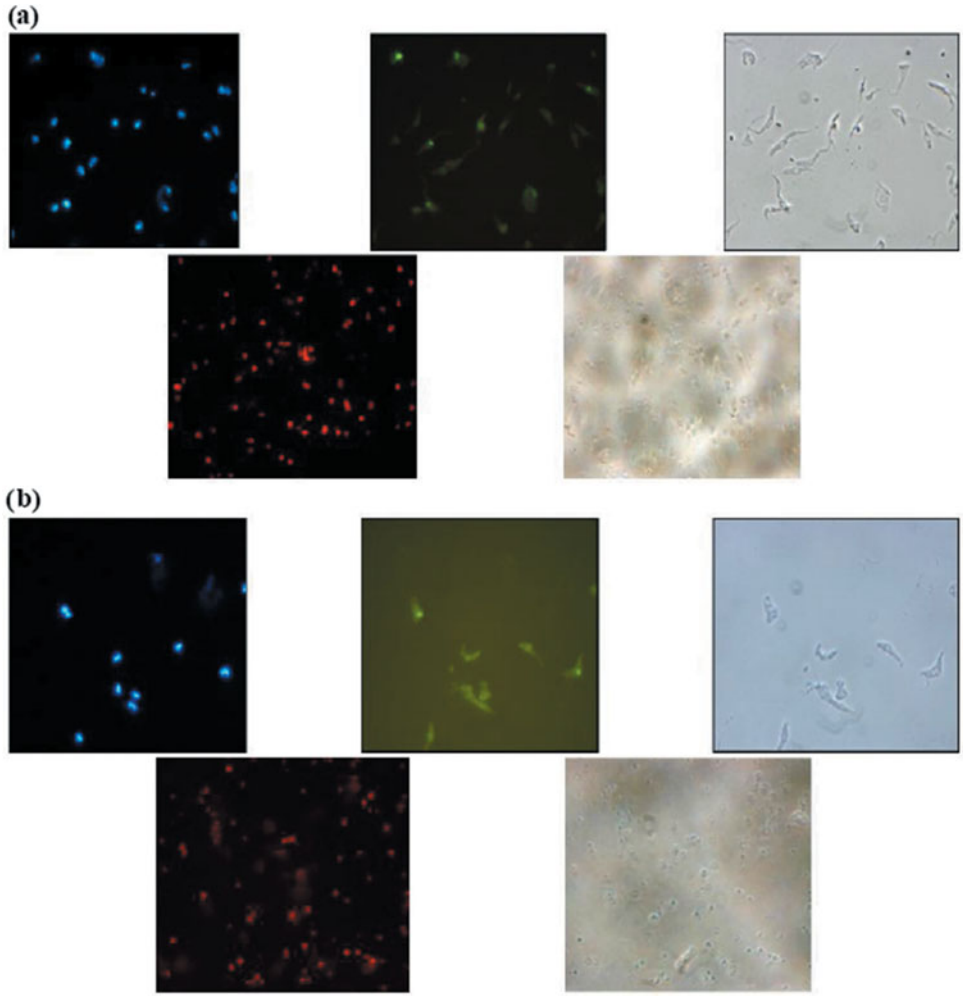

Fig. 7. Examples of results from the TUNEL and PI-staining assays (Up: left, DAPI-staining; centre, FITC-staining; right, phase contrast; 1000×. Down: left, PI-staining; right, phase contrast; 400×). (a) Treatment with **Qx1** (8 μM, 24 h); (b) Treatment with **Qx2** (18 μM, 3 h).

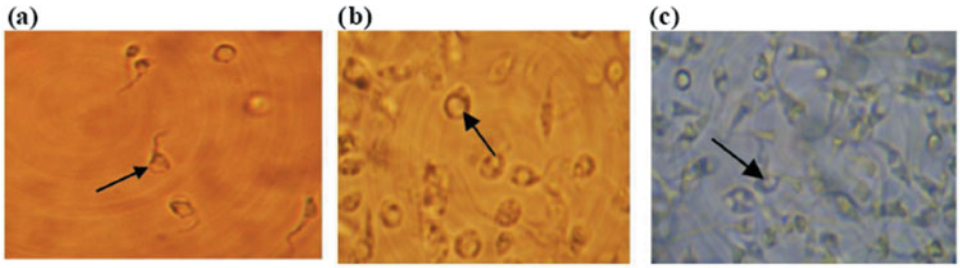

Fig. 8. Light microscopy (640×). (a) Treatment with **Fx1** (50 μM, 24 h); (b) Treatment with **Bfx1** (65 μM, 24 h); (c) Treatment with **Nf1** (5·1 μM, 24 h). Notes: epimastigotes of *T. cruzi* Tulahuen 2 strain; the arrows show the cytoplasmic vacuole.

N-oxides and cell death phenotype

^{1}H NMR-VML spectroscopy analysis of T. cruzi *epimastigotes treated with* N*-oxides.* Increased methylene resonances in ^{1}H NMR spectra resulting from the accumulation of VMLs correlate with the onset of apoptosis in several drug-treated cell models (Blankenberg *et al.* 1996) reflected in an increase in the CH_2/CH_3-ratio (Mikhailenko *et al.* 2005) and in some cases an increment in the signals from PUFA (Hakumäki *et al.* 1999). The modification of signals from choline (Cho), phosphatidylcholine (PTC) and phosphocholine (PC) has been associated with apoptosis and cell loss (Milkevitch *et al.* 2005). Additionally, apoptotic processes in *T. cruzi* epimastigotes can be visualized through modifications in the VML profiles. Thus, the increment on the CH_2/CH_3-ratio and changes in the 'choline region signals' were indicative of apoptosis while necrosis was associated, in some cases, with changes on the

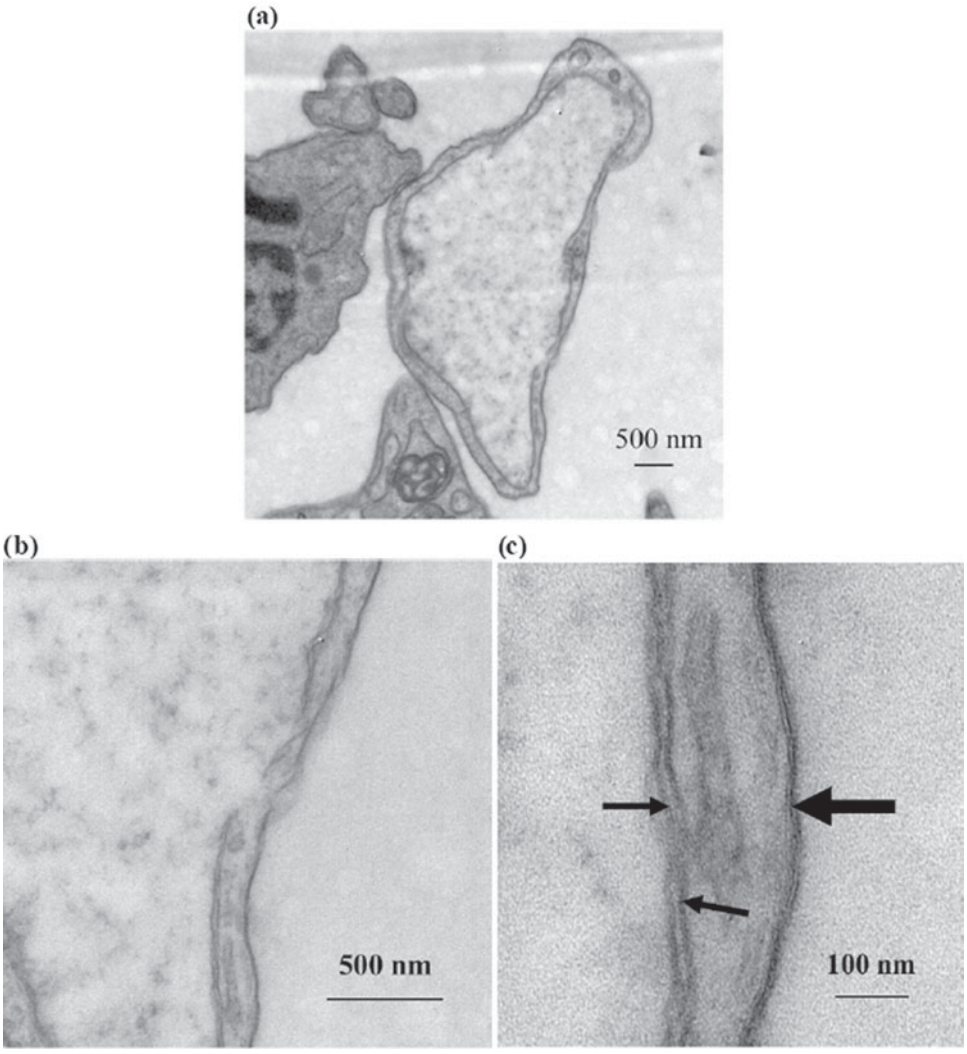

Fig. 9. Transmission electron microscopy of parasites treated with **Fx1**. (a) 12 000×; (b) Detail of (a) (40 000×); (c) Detail of (b) (200 000×). Note: big arrow: plasmatic membrane; small arrows: double membrane of vesicle.

'choline region signals'; no modifications were observed in autophagic cell-death processes (Benítez *et al*. 2012).

Table 2 summarizes the effect of the studied compounds on cell death processes as measured by ^{1}H NMR-VMLs. Experimental conditions were determined for each compound by light microscopy observation, trypan blue staining, mobility and morphology. For all the *N*-oxides, except **Qx1**, the CH_2/CH_3 ratios were statistically lower than 1·0, indicating absence of cell death by apoptosis (Benítez *et al*. 2012). Despite this, the results for **Fx2** from the PUFAs and choline-containing lipids protons data were reminiscent of those we observed previously for apoptotic conditions (Benítez *et al*. 2012). On the other hand, the same protonic regions indicate that **Qx2** induces a necrotic process, similar to the one previously observed for **Nfx** (Benítez *et al*. 2012). Both benzofuroxans, **Bfx1** and **Bfx2**, produced an increment of protons from choline-moiety. Finally, **Fx1**, **Fx3** and **Nf1** did not modify the protons signals from 'choline' and 'PUFAs' regions suggesting an autophagic process (Benítez *et al*. 2012).

In order to better clarify the type of cell death induced by *N*-oxides we applied TUNEL and PI-staining techniques on epimastigotes treated with the studied compounds.

TUNEL and PI-staining assays. Treatment of epimastigotes with the different *N*-oxides did not induce positive TUNEL results (Fig. 6, Table S1) confirming that any of those compounds induce parasite apoptosis under the assayed conditions. These results were in agreement with those obtained measuring the CH_2/CH_3 ratios by ^{1}H NMR-VML. On the other hand, PI-staining experiments showed that *N*-oxides **Fx2**, **Qx1** and **Qx2**, similarly to Nfx (Benítez *et al*. 2012), induced parasite necrosis under the same conditions applied in the ^{1}H NMR experiments (Table 2) (see examples in Fig. 7).

In addition, these experiments confirmed that neither apoptosis nor necrosis were operative, as the

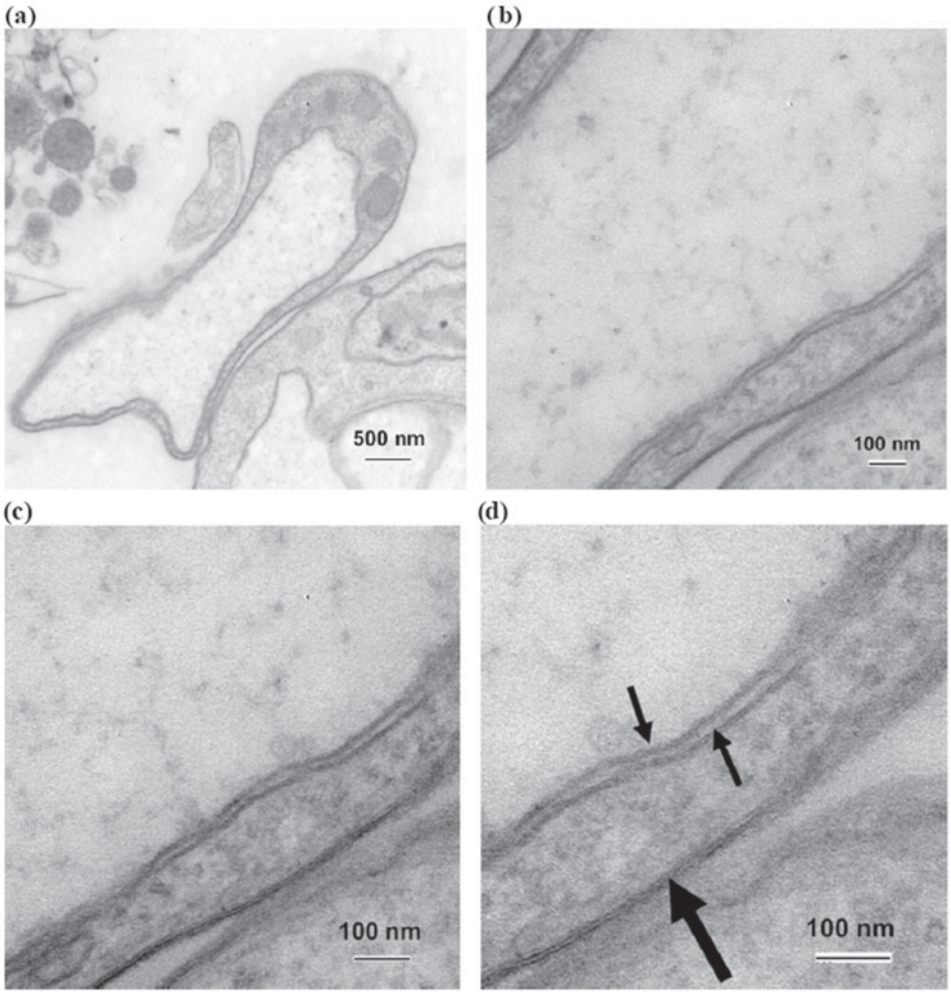

Fig. 10. Transmission electron microscopy of parasites treated with **Nf1**. (a) 25 000×; (b) Detail of (a) (100 000×); (c) Detail of (b) (150 000×); (d) Detail of (c) (200 000×). Note: big arrow: plasmatic membrane; small arrows: double membrane of vesicle.

main cell death phenotype, for *N*-oxides **Fx1**, **Bfx1**, **Bfx2** and the nitrofurane **Nf1**.

Ultrastructural characterization of cell death phenotypes in parasites treated with N-oxide compounds. Light microscopy observation of *T. cruzi* epimastigotes treated with **Fx1**, **Bfx1** and **Nf1** compounds showed a common pattern of structural changes (Fig. 8). Particularly, a big vacuole was observed in the parasitic cytoplasm. Consequently, we selected these three compounds to perform ultrastructural analysis by TEM.

Transmission electron microscopy analysis of *T. cruzi* epimastigotes treated with **Fx1** showed important ultrastructural changes, the most relevant being a big cytoplasmic vesicle, with low matrix electron density and concentric double membranes (Fig. 9). This morphology resembles the autophagic phenotype observed by the action of some naphthoimidazoles (Menna-Barreto *et al*. 2009*b*) and the 'BigEye' phenotype observed in bloodstream forms of *T. brucei* when endocytosis is disrupted by the knockdown of clathrin heavy chain (Allen *et al*. 2003; Frearson *et al*. 2010). Similarly, the nitrofurane **Nf1** induced concentric membrane structures surrounded, in some cases, by endoplasmic reticulum (Fig. 10). Contrarily, the benzofuroxane **Bfx1** showed a clear autophagic pattern, such as concentric membrane structures and autophagosomes surrounded by endoplasmic reticulum (Fig. 11).

*Evaluation of autophagy induced by the N-oxides **Fx1, Bfx1** and the nitrofurane **Nf1***. It is well-known that autophagic cell death can be inhibited by suppressing autophagosome formation with autophagic inhibitors, such as 3-methyladenine (3-mA), a non-specific inhibitor of a class III phosphatidylinositol 3-kinases required for autophagy (Klionsky *et al*. 2012). The pre-incubation of epimastigotes with 3-mA reversed the trypanosomicidal effect of the *N*-oxide **Bfx1** and the nitrofurane **Nf1** at least during the first 2 days of the studies (Fig. 12a). Probably, the effect of 3-mA was not evident from the third day as a result of the

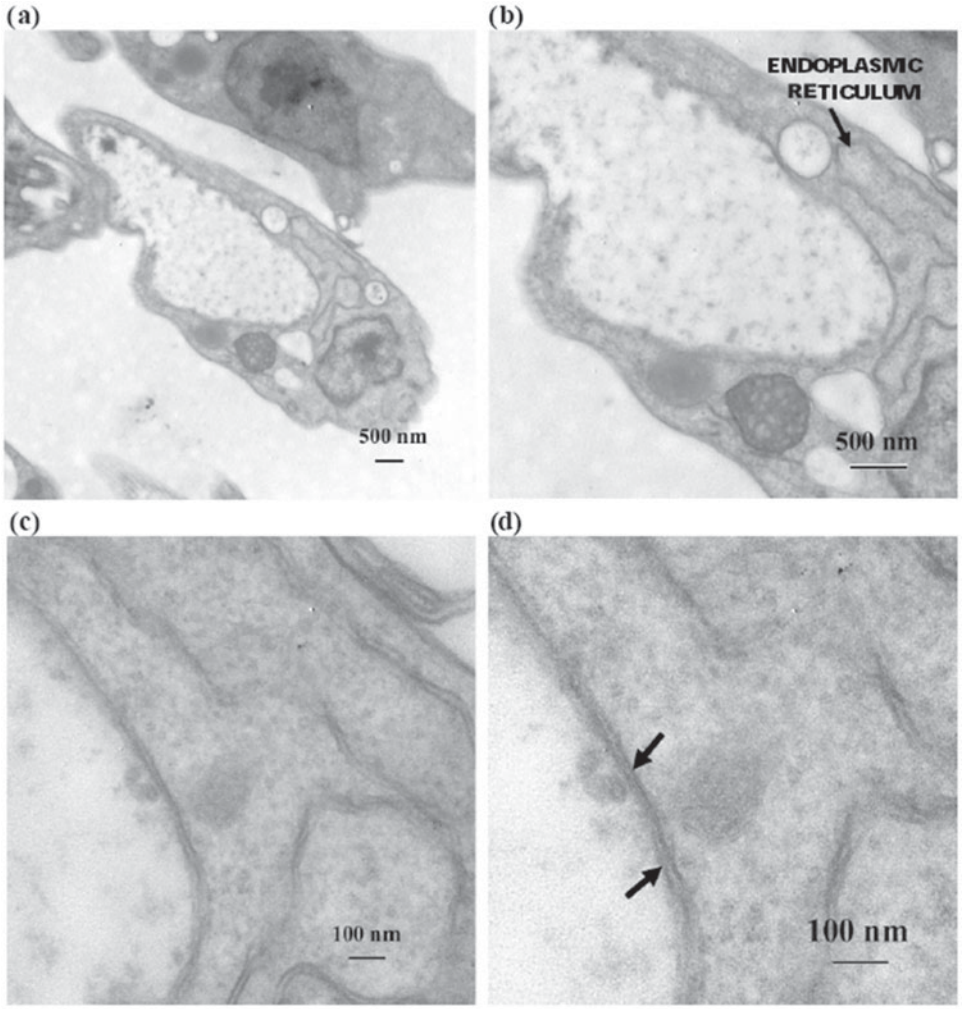

Fig. 11. Transmission electron microscopy of parasites treated with **Bfx1**. (a) 15 000×; (b) Detail of (a) (30 000×); (c) Detail of (b) (100 000×); (d) Detail of (b) (150 000×). Note: arrows: double membrane of vesicle.

parasite inhibitor consumption. 3-mA per se did not interfere with the number of parasites (data not shown). On the other hand, there was no alteration in the parasite survival percentages when 3-mA-pre-incubated parasites were treated with **Fx1** at two different doses (Fig. 12b).

DISCUSSION

Many efforts have been made to identify the mechanism of action of anti-*T. cruzi* agents. Our interest focused on studying the mode of action of the most relevant *N*-oxide-containing heterocycles from our in-house chemical library. It was previously described that some benzo[1,2-*c*][1,2,5]oxadiazole *N*-oxides (benzofuroxans) and quinoxaline N^1,N^4-dioxides were strong inhibitors of parasite dehydrogenase activity. Aiming to discriminate the mechanism of action by some of these families of compounds, levels of parasitic low-molecular weight thiols, reactive oxidant species, mitochondrial membrane potential and excreted catabolites were studied previously (Boiani *et al*. 2010; Benítez *et al*. 2011).

Most of the studied *N*-oxides decreased the release of both succinate and acetate suggesting that those compounds are acting on the mitochondria. Therefore we focused our study on the effect of *N*-oxides on mitochondrial dehydrogenases. None of the newly studied *N*-oxides were able to affect these dehydrogenases, though the quinoxalines **Qx1** and **Qx2**, as well as **Nf1**, the nitrofurane used as reference, inhibited that enzyme. Considering that these compounds present similar IC_{50} against *T. cruzi* epimastigotes but different behaviour on mitochondrial dehydrogenases, and taking into account that the metabolism of carboxylic acids is related to glucose metabolism (Cazzulo, 1992; Coustou *et al*. 2005), we analysed glucose consumption by the parasite in the presence of this *N*-oxide. This study may be indicating that **Qx2** also affects the integrity or some pathway into the glycosome (Bringaud *et al*. 2006; Opperdoes and Coombs, 2007).

Several efforts have been made to identify the type of cell death in parasitic protozoa (Rodrigues and De Souza, 2008) but none with regard to *N*-oxides.

Both mobile lipids analysed by ^{1}H NMR (Benítez *et al*. 2012) and TUNEL assay showed that the

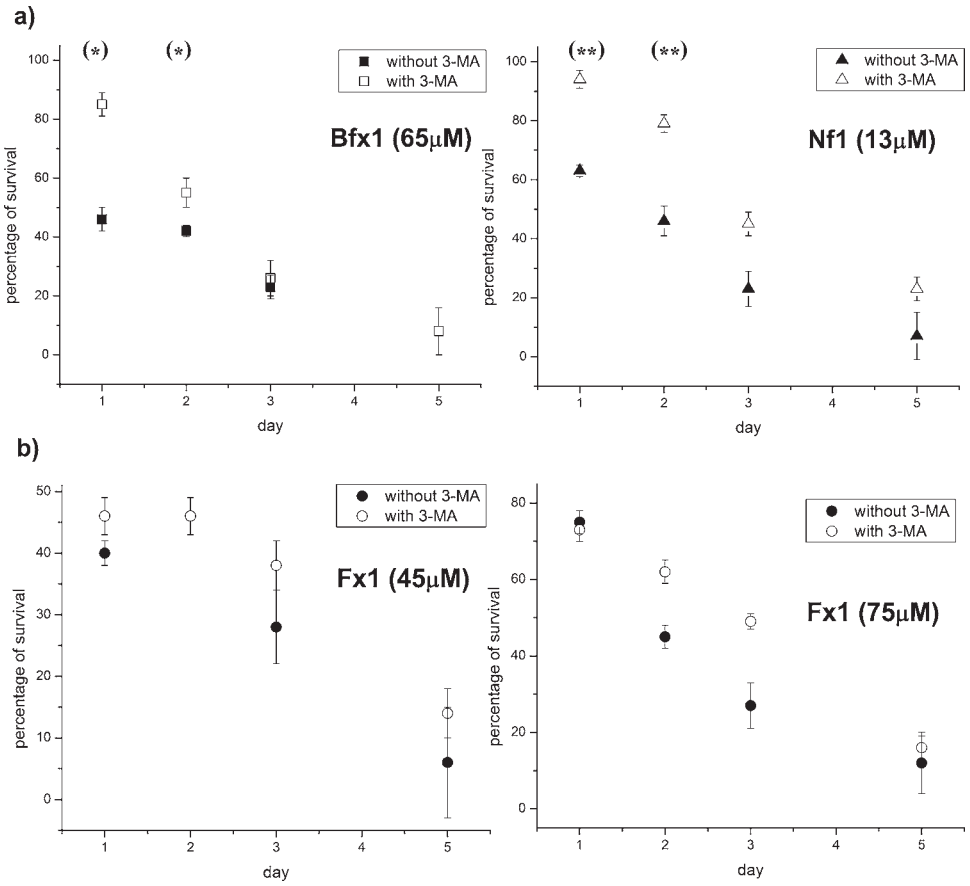

Fig. 12. Pre-incubation of **Bfx1**-, **Nf1**-, and **Fx1**-treated epimastigotes with protease inhibitor 3-MA. Data represent the mean ± S.D. of at least three independent experiments. (*) $P < 0{\cdot}003$; (**) $P < 0{\cdot}0003$.

studied *N*-oxides do not induce *T. cruzi* death by apoptosis under the assayed conditions. However, according to propidium iodide staining both quinoxaline dioxides, **Qx1** and **Qx2** as well as the 1,2,5-oxadiazole *N*-oxide **Fx2** and the clinically used nitrofurane, Nifurtimox, were able to induce necrosis of parasites in the assayed conditions.

Light microscopy observations indicated that the **Fx2**-structurally related *N*-oxides **Fx1** and **Bfx1**, together with the nitrofurane **Nf1**, induced very particular structural changes. This is interesting considering that structural similarities in these families of compounds are not related to the type of cellular death. Therefore, we performed ultrastructural analysis by TEM and the use of protease inhibitor to confirm or discard an autophagy process. Autophagy is a self-degradation process presented in eukaryotes, implicated in the removal and/or remodelling of damaged cellular structures. In yeasts and mammals, autophagosome formation involves the assembling of a pre-autophagosomal structure, close to endoplasmic reticulum cisternae (Yorimitsu and Klionsky, 2007).

Ultrastructural analysis and pre-incubation with the protease-inhibitor 3-methyladenine suggested the induction of an autophagic phenotype in *T. cruzi* epimastigotes treated with **Bfx1** and **Nf1**. Morphological characteristics such as the appearance of concentric membrane structures and autophagosome-like bodies were commonly observed in treated parasites, with the latter surrounded by endoplasmic reticulum. Additionally, the pre-incubation of epimastigotes with the autophagic inhibitor abolished the effect of **Bfx1** and **Nf1**, at least for 48 h. However, the ultrastructural and protease-inhibitor data showed a very different behaviour for **Fx1**. In this case, the presence of a concentric membrane vesicle, such as an autophagosome, could indicate an autophagic phenotype; however, endoplasmic reticulum in close proximity to the vacuole was not observed. Additionally, there was no effect of the inhibitor 3-methyladenine in parasite survival. Consequently, a 'BigEye' phenotype may be proposed as a consequence of **Fx1** action, as observed in *T. brucei* bloodstream forms when endocytosis is disrupted by the knockdown of clathrin heavy chain (Allen *et al*. 2003; Frearson *et al*. 2010). However, to consider that this process is operative in **Fx1** treated *T. cruzi* epimastigotes needs further investigation.

Our results in *T. cruzi* treated with different classes of *N*-oxides has led to an understanding of mechanism of action and protozoa cell death that could help develop new therapeutic strategies.

SUPPLEMENTARY MATERIAL

To view supplementary material for this article, please visit http://dx.doi.org/S003118201300200X.

FINANCIAL SUPPORT

This work was supported by CSIC-Grupos 611 (Uruguay), PEDECIBA (Uruguay), FONDECYT 1090124 and 1130113 (to NG), FONDECYT 1110053 (to GC), CONICYT-PBCT Anillo ACT 112 'Research in the Design of Pharmacological and Immunological Strategies for the Control of Parasitic and Neoplasic Aggressions' (Chile), and RIDIMEDCHAG-CYTED. D.B. is a fellow of ANII.

REFERENCES

Allen, C. L., Goulding, D. and Field, M. C. (2003). Clathrin-mediated endocytosis is essential in *Trypanosoma brucei*. *EMBO Journal* **22**, 4991–5002.

Alvarez, V. E., Kosec, G., Sant'Anna, C., Turk, V., Cazzulo, J. J. and Turk, B. (2008*a*). Autophagy is involved in nutritional stress response and differentiation in *Trypanosoma cruzi*. *Journal of Biological Chemistry* **283**, 3454–3464.

Alvarez, V. E., Kosec, G., Sant'Anna, C., Turk, V., Cazzulo, J. J. and Turk, B. (2008*b*). Blocking autophagy to prevent parasite differentiation. A possible new strategy for fighting parasitic infections? *Autophagy* **4**, 361–363.

Aravena, C. M., Olea-Azar, C., Cerecetto, H., González, M., Maya, J. D. and Rodríguez-Becerra, J. (2011). Potent 5-nitrofuran derivatives inhibitors of *Trypanosoma cruzi* growth: electrochemical, spectroscopic and biological studies. *Spectrochimica Acta A Molecular Biomolecular Spectroscopy* **79**, 312–319.

Benítez, D., Cabrera, M., Hernández, P., Boiani, L., Lavaggi, M. L., Di Maio, R., Yaluff, G., Serna, E., Torres, S., Ferreira, M. E., Vera de Bilbao, N., Torres, E., Pérez-Silanes, S., Solano, B., Moreno, E., Aldana, I., López de Ceráin, A., Cerecetto, H., González, M. and Monge, A. (2011). 3-Trifluoromethylquinoxaline *N,N'*-dioxides as anti-trypanosomatid agents. Identification of optimal anti-*T. cruzi* agents and mechanism of action studies. *Journal of Medicinal Chemistry* **54**, 3624–3636.

Benítez, D., Pezaroglo, H., Martínez, V., Casanova, G., Cabrera, G., Galanti, N., González, M. and Cerecetto, H. (2012). Study of *Trypanosoma cruzi* epimastigote cell death by NMR-visible mobile lipid analysis. *Parasitology* **139**, 506–515.

Blankenberg, F. G., Storrs, R. W., Naumovski, L., Goralski, T. and Spielman, D. (1996). Detection of apoptotic cell death by proton nuclear magnetic resonance spectroscopy. *Blood* **87**, 1951–1956.

Boiani, L., Aguirre, G., González, M., Cerecetto, H., Chidichimo, A., Cazzulo, J. J., Bertinaria, M. and Guglielmo, S. (2008). Furoxan-, alkylnitrate-derivatives and related compounds as anti-trypanosomatid agents: mechanism of action studies. *Bioorganic and Medicinal Chemistry* **16**, 7900–7907.

Boiani, M., Boiani, L., Alicia, A., Hernández, P., Chidichimo, A., Cazzulo, J. J., Cerecetto, H. and González, M. (2009). Second generation of 2*H*-benzimidazole 1,3-dioxide derivatives as anti-trypanosomatid agents: synthesis, biological evaluation, and mode of action studies. *European Journal of Medicinal Chemistry* **44**, 4426–4433.

Boiani, M., Piacenza, L., Hernández, P., Boiani, L., Cerecetto, H., González, M. and Denicola, A. (2010). Mode of action of nifurtimox and N-oxide-containing heterocycles against *Trypanosoma cruzi*: is oxidative stress involved? *Biochemical Pharmacology* **79**, 1736–1745.

Bringaud, F., Rivière, L. and Coustou, V. (2006). Energy metabolism of trypanosomatids: adaptation to available carbon sources. *Molecular and Biochemical Parasitology* **149**, 1–9.

Caterina, M. C., Perillo, I. A., Boiani, L., Pezaroglo, H., Cerecetto, H., González, M. and Salerno, A. (2008). Imidazolidines as new anti-*Trypanosoma cruzi* agents: biological evaluation and structure-activity relationships. *Bioorganic and Medicinal Chemistry* **16**, 2226–2234.

Cazzulo, J. J. (1992). Aerobic fermentation of glucose by trypanosomatids. *FASEB Journal* **6**, 3153–3161.

Cerecetto, H. and González, M. (2008). Anti-*T. cruzi* agents: our experience in the evaluation of more than five hundred compounds. *Mini Review in Medicinal Chemistry* **8**, 1355–1383.

Cerecetto, H. and González, M. (2010). Synthetic medicinal chemistry in Chagas' disease: compounds at the final stage of "Hit-to-Lead" phase. *Pharmaceuticals* **3**, 810–838.

Coustou, V., Besteiro, S., Rivière, L., Biran, M., Biteau, N., Franconi, J. M., Boshart, M., Baltz, T. and Bringaud, F. (2005). A mitochondrial NADH-dependent fumarate reductase involved in the production of succinate excreted by procyclic *Trypanosoma brucei*. *Journal of Biological Chemistry* **280**, 16559–16570.

De Castro, S. L. and Meirelles, M. N. (1990). Mechanism of action of a nitroimidazole thiadiazole derivative upon *Trypanosoma cruzi* tissue culture amastigotes. *Memórias do Instituto Oswaldo Cruz* **85**, 95–99.

Fernandez-Ramos, C., Luque, F., Fernández-Becerra, C., Osuna, A., Jankevicius, S. I., Jankevicius, V., Rosales, M. J. and Sánchez-Moreno, M. (1999). Biochemical characterisation of flagellates isolated from fruits and seeds from Brazil. *FEMS Microbiology Letters* **170**, 343–348.

Frearson, J. A., Brand, S., McElroy, S. P., Cleghorn, L. A. T., Smid, O., Stojanovski, L., Price, H. P., Guther, M. L. S., Torrie, L. S., Robinson, D. A., Hallyburton, I., Mpamhanga, C. P., Brannigan, J. A., Wilkinson, A. J., Hodgkinson, M., Hui, R., Qiu, W., Raimi, O. G., van Aalten, D. M. F., Brenk, R., Gilbert, I. H., Read, K. D., Fairlamb, A. H., Ferguson, M. A. J., Smith, D. F. and Wyatt, P. G. (2010). *N*-myristoyltransferase inhibitors as new leads to treat sleeping sickness. *Nature* **464**, 728–734.

González, M. and Cerecetto, H. (2011). Novel compounds to combat trypanosomatid infections: a medicinal chemical perspective. *Expert Opinion on Therapeutic Patents* **21**, 699–715.

Hakumäki, J. M., Poptani, H., Sandmair, A. M., Ylä-Herttuala, S. and Kauppinen, R. A. (1999). ^{1}H MRS detects polyunsaturated fatty acid accumulation during gene therapy of glioma: implications for the *in vivo* detection of apoptosis. *Nature Medicine* **5**, 1323–1327.

Hernández, P., Rojas, R., Gilman, R. H., Sauvain, M., Lima, L. M., Barreiro, E. J., González, M. and Cerecetto, H. (2013). Hybrid furoxanyl *N*-acylhydrazone derivatives as hits for the development of neglected diseases drug candidates. *European Journal of Medicinal Chemistry* **59**, 64–74.

Irigoín, F., Inada, N. M., Fernandes, M. P., Piacenza, L., Gadelha, F. R., Vercesi, A. E. and Radi, R. (2009). Mitochondrial calcium overload triggers complement-dependent superoxide-mediated programmed cell death in *Trypanosoma cruzi*. *Biochemical Journal* **418**, 595–604.

Jiménez, V., Paredes, R., Sosa, M. A. and Galanti, N. (2008). Natural programmed cell death in *T. cruzi* epimastigotes maintained in axenic cultures. *Journal of Cellular Biochemistry* **105**, 688–698.

Klionsky, D. J., Abdalla, F. C., Abeliovich, H., Abraham, R. T., Acevedo-Arozena, A., Adeli, K., Agholme, L., *et al.* (2012). Guidelines for the use and interpretation of assays for monitoring autophagy. *Autophagy* **8**, 445–544.

Maarouf, M., De Kouchkovsky, Y., Brown, S., Petit, P. X. and Robert-Gero, M. (1997). *In vivo* interference of paromomycin with mitochondrial activity of *Leishmania*. *Experimental Cell Research* **232**, 339–348.

MacKenzie, S. H. and Clark, A. C. (2008). Targeting cell death in tumors by activating caspases. *Current Cancer Drug Targets* **8**, 98–109.

Menna-Barreto, R. F., Salomão, K., Dantas, A. P., Santa-Rita, R. M., Soares, M. J., Barbosa, H. S. and de Castro, S. L. (2009*a*). Different cell death pathways induced by drugs in *Trypanosoma cruzi*: an ultrastructural study. *Micron* **40**, 157–168.

Menna-Barreto, R. F., Corrêa, J. R., Cascabulho, C. M., Fernandes, M. C., Pinto, A. V., Soares, M. J. and de Castro, S. L. (2009*b*). Naphthoimidazoles promote different death phenotypes in *Trypanosoma cruzi*. *Parasitology* **136**, 499–510.

Menna-Barreto, R. F. S., Beghini, D. G., Ferreira, A. T. S., Pinto, A. V., De Castro, S. L. and Perales, J. (2010). A proteomic analysis of the mechanism of action of naphthoimidazoles in *Trypanosoma cruzi* epimastigotes *in vitro*. *Journal of Proteomics* **73**, 2306–2315.

Merlino, A., Benítez, D., Chavez, S., Da Cunha, J., Hernández, P., Tinoco, L. W., Campillo, N. E., Páez, J. A., Cerecetto, H. and González, M. (2010). Development of second generation amidinohydrazones, thio- and semicarbazones as *Trypanosoma cruzi*-inhibitors bearing benzofuroxan and benzimidazole 1,3-dioxide core scaffolds. *Medicinal Chemistry Communications* **1**, 216–228.

Mesa-Valle, C. M., Castilla-Calvente, J., Sánchez-Moreno, M., Moraleda-Lindez, V., Barbe, J. and Osuna, A. (1996). Activity and mode of action of acridine compounds against *Leishmania donovani*. *Antimicrobial Agents and Chemotherapy* **40**, 684–690.

Mikhailenko, V. M., Philchenkov, A. A. and Zavelevich, M. P. (2005). Analysis of ^{1}H NMR-detectable mobile lipid domains for assessment of

apoptosis induced by inhibitors of DNA synthesis and replication. *Cell Biology International* **29**, 33–39.

Milkevitch, M., Shim, H., Pilatus, U., Pickup, S., Wehrle, J. P., Samid, D., Poptani, H., Glickson, J. D. and Delikatny, E. J. (2005). Increases in NMR-visible lipid and glycerophosphocholine during phenylbutyrate-induced apoptosis in human prostate cancer cells. *Biochimica et Biophysica Acta* **1734**, 1–12.

Opperdoes, F. R. and Coombs, G. H. (2007). Metabolism of *Leishmania*: proven and predicted. *Trends in Parasitology* **23**, 149–158.

Rodrigues, J. C. and De Souza, W. (2008). Ultrastructural alterations in organelles of parasitic protozoa induced by different classes of metabolic inhibitors. *Current Pharmaceutical Design* **14**, 925–938.

Ricci, M. S. and Zong, W. X. (2006). Chemotherapeutic approaches for targeting cell death pathways. *Oncologist* **11**, 342–357.

Sánchez-Moreno, M., Fernández-Becerra, C., Castilla, J. and Osuna, A. (1995). Metabolic studies by ^{1}H NMR of different forms of *Trypanosoma cruzi* as obtained by '*in vitro*' culture. *FEMS Microbiology Letters* **133**, 119–125.

Sánchez-Moreno, M., Gómez-Contreras, F., Navarro, P., Marín, C., Ramírez-Macías, I., Olmo, F., Sanz, A. M., Campayo, L., Cano, C. and Yunta, M. J. (2012). *In vitro* leishmanicidal activity of imidazole- or pyrazole-based benzo[*g*]phthalazine derivatives against *Leishmania infantum* and *Leishmania braziliensis* species. *Journal of Antimicrobial Chemotherapy* **67**, 387–397.

Tan, T. T. and White, E. (2008). Therapeutic targeting of death pathways in cancer: mechanisms for activating cell death in cancer cells. *Advances in Experimental Medicine and Biology* **615**, 81–104.

WHO. (2013). http://www.who.int/neglected_diseases/diseases/chagas/en/index.html.

Yorimitsu, T. and Klionsky, D. J. (2007). Eating the endoplasmic reticulum: quality control by autophagy. *Trends in Cell Biology* **17**, 279–285.